Influence mechanism of surface hardness of soil samples on plasma

Yutao Huang
Changchun University of Technology
Jingjun Lin
Changchun University of Technology
Xiaomei Lin (187049860@qq.com)
Changchun University of Technology

Research Article

Keywords: laser-induced breakdown spectroscopy (LIBS), surface hardness, plasma temperature, calibration curve

Posted Date: May 11th, 2022

DOI: https://doi.org/10.21203/rs.3.rs-1629822/v1

Abstract

Laser-induced breakdown spectroscopy (LIBS) can be used to quantitatively analyze heavy metal elements in soil, but the matrix effects have always been an important problem affecting the accuracy of quantitative analysis. The influence mechanism of matrix effects on plasma needs to be further studied. In this paper, the main purpose is to analyze the influence mechanism of sample surface hardness on plasma. The trend of plasma temperature, the ratio of ion line to atomic line of Cr and Cu elements, and the calibration curve of Cr and Cu elements with the change of sample surface hardness are analyzed, respectively. The results show that the plasma temperature and the ratio of ion line to atomic line of Cr and Cu elements increase with the increase of sample surface hardness. Meanwhile, the root mean square error (RMSE) and average relative error (ARE) of Cr and Cu elements in the samples with a hardness of 98HA are lower than those of the samples with a hardness of 43HA and 70HA. For samples with a surface hardness of 98HA, the RMSE and ARE of Cr are 0.027wt% and 9.763%, and those of Cu are 0.047wt% and 15.862%, respectively. However, the stability of the training data decreases with the surface hardness increases. The relative standard deviations (RSD) of Cr and Cu elements are 19.383% and 34.383%, respectively, for samples with a surface hardness of 98HA. By studying the influence of sample surface hardness on plasma temperature and calibration curve, the influence mechanism of sample surface hardness on plasma was explored.

Introduction

Heavy metal pollution in soil has attracted more and more attention[1]. How to quickly and accurately detect the heavy metal content in soil is an important problem. Conventional methods such as atomic absorption spectroscopy (AAS), inductively coupled plasma atomic emission spectrometry (ICP-AES)[2, 3, 4, 5, 6], etc., require complex sampling and sample pretreatment processes[7], and these methods face challenges such as long detection cycle, low detection efficiency, and inability to achieve in-situ online detection. Nowadays, laser-induced breakdown spectroscopy (LIBS), as a rapid spectral analysis technology without sample processing, is gradually applied to detection of heavy metal in soil. However, the application of LIBS to the quantitative analysis of heavy metals in soil still faces many problems, such as matrix effects, self-absorption effect and so on[8, 9, 10]. Matrix effect is one of the important factors affecting the accuracy of quantitative analysis of heavy metals in soil[11]. In particular, the soil composition is complex, and it is difficult to maintain the consistency of the test sample and the standard sample in terms of temperature, humidity, and surface hardness. When the matrix of the standard sample is different from that of the sample to be tested, the calibration model established with the standard sample is difficult to apply to the test sample, which brings great difficulties to the quantitative analysis of heavy metals in soil. Zaytsev et al.[12] investigated the effect of UV laser radiation (355 and 266 nm) on reducing matrix effects. The results indicate that the laser wavelength of 355nm can more effectively reduce the influence of the matrix effects on quantitative analysis, and the best calibration model can be obtained. And then, quantitative analysis of Pb elements in unknown samples was carried out, and the results are similar to those of XRF. Yi et al.[2] proposed a standard addition method to reduce matrix

effects after removing the background signal based on wavelet transform algorithm. The results show that the method can effectively reduce the root mean square error of prediction of Pb in soil from 303ppm to 25.7ppm. Wang et al.[13] proposed a multivariate analysis method combining least absolute shrinkage and selection operator with principal component regression. The researches show that the method can effectively reduce matrix interference and has stable prediction performance. The normalized root mean square error of Cu, Ni, Cr, Pb are 6.84%, 8.87%, 9.71% and 10.76%, respectively. Most of the above studies focus on the reduction and correction of matrix effects, while the mechanism of matrix effects on plasma is rarely involved. In order to more effectively reduce the influence of matrix effects in soil on the accuracy of quantitative analysis, it is necessary to conduct more in-depth research on the influence mechanism of matrix effects on plasma.

In this paper, we mainly study the influence mechanism of surface hardness on plasma. In order to diagnose the change of plasma with sample surface hardness, plasma temperature and the ratio of ion line to atomic line of Cr and Cu elements were calculated. At the same time, the limit of detection(LOD) of Cr and Cu elements, the root mean square error(RMSE), the average relative error(ARE), and the relative standard deviation(RSD) of the training set of Cr and Cu elements were calculated to explore the influence of sample surface hardness on calibration curve.

Experiments And Methods

Experimental setup

A schematic diagram of the experimental setup is shown in Fig. 1. The light source of the experiment was a Q-switched Nd: YAG laser (laser wavelength, 1064nm; pulse energy, 50mJ; pulse width, 8ns; repetition rate, 1Hz; and Nimma-400, Beamtech). The plasma was generated by focusing the laser beam onto the sample surface with a focus lens (f = 120mm). The laser energy of ablated samples was regulated by an energy attenuation system consisting of a half-wave plate and a glan prism. And plasma signal was collected by two plano-convex lenses, and then the emission spectra was coupled to an echelle spectrometer (spectral range, 200-975nm; resolution, $\lambda/\Delta\lambda = 5000$; and Me5000, Andor) equipped with an intensified charge-coupled device (ICCD) camera for spectrum processing. The ICCD and laser were triggered synchronously by a digital pulse generator (BNC575, Berkeley Nucleonics Corp). In order to investigate the influence of surface hardness on ablation craters, the ablation craters map was obtained by an electron microscope. The following experiments were carried out under these conditions.

Sample Preparation

The samples used in this experiment are a mixture of standard soil GBW07403, crystalline $Cr(NO_3)_3 \cdot 9H_2O$, and crystalline $Cu(NO_3)_2 \cdot 3H_2O$ according to a certain proportion. The initial concentration of Cr and Cu in the standard sample is very low about 2.28 μg and 6.4 μg, which is essentially negligible in comparison with the added concentration. The standard soil was mixed with $Cr(NO_3)_3 \cdot 9H_2O$ and $Cu(NO_3)_2 \cdot 3H_2O$ in a

mortar, deionized water was added to the mortar, and the mixture was completely stirred. Then the mixed samples were dried, ground, and sifted to obtain a powder mixture with a small enough particle size. The 3g powder samples were placed into the mold, and pressure of 10MPa, 20MPa and 30MPa were applied to each concentrated sample, respectively, for 30min to obtain a pellet with different surface hardness with a diameter of 30mm, and a thickness of 2mm. The surface hardness of samples was measured by shore hardness tester, and the specific parameters of the samples are shown in Table 1.

Table 1
Specific parameters of samples used in the experiment

Sample number	Cr concentration (wt%)	Cu concentration (wt%)	Pressure (MPa)	Hardness (HA)
S1	0.1	0.1	10	43
S2	0.2	0.2		
S3	0.3	0.3		
S4	0.4	0.4		
S5	0.5	0.5		
S6	0.1	0.1	20	70
S7	0.2	0.2		
S8	0.3	0.3		
S9	0.4	0.4		
S10	0.5	0.5		
S11	0.1	0.1	30	98
S12	0.2	0.2		
S13	0.3	0.3		
S14	0.4	0.4		
S15	0.5	0.5		

Results And Discussion

Spectral line selection

In this paper, the spectra in the range of 300-600nm were collected, and the Cr and Cu elements in the samples used in the experiment were analyzed. The characteristic spectral lines of Cr and Cu elements were identified by combining the information from the National Institute of Standards and Technology (NIST) database, the collected spectral information and the spectral line recognition software. And

atomic lines Cr I 425.44nm, Cr I 427.48nm, Cr I 428.97, Cr I 520.84nm, Cu I 4.75nm, and ionic lines Cr II 405.41nm, Cu II 368.65nm were analyzed, respectively. At the same time, in order to reduce the influence of environmental fluctuation and system error on the detection results, 20 sample points were collected for each sample, and the average value of 5 spectra was taken as the final result for each sample point. One spectrum in the experimental acquisition spectrum is shown in Fig. 2.

Effect Of Surface Hardness On Plasma Temperature

Under the assumption of local thermodynamic equilibrium (LTE)[14], the Cr element was used as the analysis element to calculate the change of plasma temperature of samples with different surface hardness[15, 16, 17]. The spectral parameters of the characteristic spectral lines used are shown in Table 2.

Table 2
Spectral parameters of Cr atomic lines

Wavelength(nm)	$A_{ki}(s^{-1})$	E_k(eV)	g_k
425.44	3.15e + 7	2.91	9
427.48	3.07e + 7	2.90	7
428.97	3.16e + 7	2.89	5
520.84	5.06e + 7	3.32	7

The calculation of plasma temperature was carried out for samples numbered S4, S9 and S14 with the same concentration of Cr elements and different surface hardness. And the plasma temperature was obtained using Boltzmann equation:

$$ln\frac{I\lambda}{g_k A_{ki}} = \frac{-E_k}{kT} + ln\frac{4\pi Z}{hcN_0} \quad (1)$$

where I is the intensity of the characteristic spectral line, λ is the wavelength of the characteristic spectral line, g_k is the statistical weight of the upper state, k is the Boltzmann constant, T is the plasma temperature, Z is the partition function, which is usually regarded as the statistical weight of the ground state, h stands for the Planck constant, c is the speed of light, and N_0 represents the population density[18]. In Eq. (1), E_k is defined as the x-axis, and $ln\frac{I\lambda}{g_k A_{ki}}$ is defined as the y-axis. The slope $-\frac{1}{kT}$ can be obtained through the known $ln\frac{I\lambda}{g_k A_{ki}}$ and E_k, and then the plasma temperature can be calculated. The corresponding relationship between plasma temperature and sample surface hardness is shown in Fig. 3.

At the same time, the ablation craters profiles of samples with different surface hardness were photographed to research the influence mechanism of surface hardness on plasma, as shown in Fig. 4.

As can be seen from Fig. 3, with the increase of sample surface hardness, the excitation temperature of plasma also increases. This may be because the ablated mass of the sample surface decreases with the increase of the sample surface hardness, which increases the absorption of laser energy by the plasma and intensifies the particles collision inside the plasma. Figure 4 proves this view. From the profile of the ablation craters in Fig. 4, it can be roughly judged that with the increase of sample surface hardness, the volume of the ablation craters decreases, and the ablated mass of the sample decreases. At the same time, the correlation coefficient (R^2) between sample surface hardness and plasma temperature can reach 0.853, which has a good linear relationship. Thus plasma temperature can be used as an evaluation index to predict sample surface hardness.

Effect Of Surface Hardness On The Ratio Of Ionic Lines To Atomic Lines

In order to study the effect of surface hardness on the atoms and ions in plasma, the trend of the ratio of ionic lines to atomic lines of Cr and Cu with surface hardness was studied with S4, S9 and S14 samples[19, 20]. The maximum and minimum values of 20 spectra of each sample were removed, and the average values of the remaining 18 spectra were taken. In this paper, the values of Cr II 405.41nm/Cr I 425.44nm and Cu II 368.65nm/Cu I 324.75nm were used as the y-axis, respectively, and the surface hardness was used as the x-axis to establish the relationship between surface hardness and the ratio of ionic to atomic lines, as shown in Fig. 5.

As can be seen from Fig. 5, with the increase of sample hardness, the ratio of ionic lines and atomic lines of Cr and Cu elements showed an upward trend. This suggests that the increase of surface hardness leads to the increase of the number of ions in the plasma. This may be because samples with higher surface hardness have stronger repulsive force. With the increase of sample surface hardness, the shock wave front speeds increases, which increases the collision probability of particles and the ionization rate of atoms. Abdel-salam et al.[21] also demonstrated that the harder the sample, the faster the shock wave and the greater the ratio of ionic lines to atomic lines. Meanwhile, the linear relationship between the surface hardness of samples and the ratio of ionic lines to atomic lines of elements can be seen that the ratio of ionic lines to atomic lines of elements can also be used as an evaluation index for hardness testing.

Effect Of Surface Hardness On The Calibration Curve

As one of the matrix effects, a change in surface hardness can affect the calibration curve. In this paper, the influence of surface hardness of samples on the calibration curves of Cr and Cu elements in samples was analyzed. Similarly, the maximum and minimum values of 20 spectra of each sample were removed,

and the remaining 18 spectra were calculated. The performance of the calibration curve was evaluated using the values of LOD, RMSE, ARE, and RSD. The calculation equation of each parameter is as follows:

$$LOD(wt\%) = \frac{3\sigma}{k} \quad (2)$$

$$RMSE(wt\%) = \sqrt{\frac{\sum_{i=1}^{N}(\hat{c}_i - c_i)^2}{N}} \quad (3)$$

$$ARE(\%) = \frac{100}{N}\sum_{i=1}^{N}\frac{|\hat{c}_i - c_i|}{c_i} \quad (4)$$

$$RSD(\%) = \frac{\sqrt{\sum_{i=1}^{n}\frac{(\hat{c}_i - \bar{c})^2}{n-1}}}{\bar{c}} \times 100 \quad (5)$$

In Eq. (2), σ is the standard deviation of the spectral background signal, and k is the slope of the calibration curve. In Eqs. (3), (4), and (5), N (= 5 in this work) represents the number of samples with the same hardness and different element concentrations, n (= 18 in this work) is the number of repeated measurements of the same sample under the same conditions. $\hat{c}_i$, c_i, $\bar{c}$ represent the predicted concentration, the actual concentration, and the average value of repeated measurements, respectively.

Figure 6 shows the calibration curves of Cr and Cu elements with different surface hardness. Among them, the R^2 of the calibration curve of Cr and Cu elements in the samples with a surface hardness of 98HA is better than that of the samples with a surface hardness of 43HA and 70HA. The evaluation parameters of the calibration curve in Fig. 6 are calculated, and the results are shown in Table 3.

Table 3
Parameter values of calibration curves of Cr and Cu elements with different surface hardness

Element	Hardness(HA)	R^2	RMSE(wt%)	ARE(%)	RSD(%)	LOD(wt%)
Cr	43	0.895	0.044	12.356	13.496	0.015
	70	0.838	0.096	26.562	16.909	0.016
	98	0.962	0.027	9.763	19.383	0.017
Cu	43	0.874	0.054	16.010	24.220	0.034
	70	0.714	0.089	27.245	32.692	0.036
	98	0.899	0.047	15.862	34.383	0.045

As can be seen from Table 3, the RMSE and ARE values of Cr and Cu calibration curves of samples with a surface hardness of 98HA are smaller than those of samples with a hardness of 43HA and 70HA, which indicates that the accuracy of Cr and Cu calibration curves with a surface hardness of 98HA is better. This is attributed to the increase of surface hardness, which reduces the ablated mass of the sample, the plasma can absorb the laser energy more fully, and the detection value is closer to the actual value. However, the RMSE and ARE values of Cr and Cu element calibration curves with a surface hardness of 70HA are relatively large, which may be the fluctuation of laser energy, resulting in a large deviation between the detection value and the actual value. In contrast to the improvement of detection accuracy, the LOD and RSD values of Cr and Cu elements of the sample with a surface hardness of 98HA become larger, indicating that the stability of detection decreases and the repeatability of experimental results decreases. It may be that the shock wave front speeds increase, which intensifies the disordered state of particle collision inside the plasma. And the background signal and noise signal fluctuate greatly, resulting in the large fluctuation of each measurement result.

Conclusion

In this paper, the influence mechanism of soil surface hardness on plasma was studied. It is found that the plasma temperature increases with the increase of soil surface hardness, which is attributed to the higher surface hardness, and the lower ablated mass of the sample. And the plasma absorbs the laser energy more fully, and then, the collision of particles inside the plasma intensifies, which eventually leads to an increase in plasma temperature. Similarly, the ratio of ion line to atomic line of Cr and Cu elements also increases with the increase of sample surface hardness. This is because the shock wave front speeds increase with the increase of sample surface hardness, the collision probability of particles in plasma increases, and then the ionization rate of atoms increases. And the influence of sample surface hardness on the calibration curve is mainly reflected in the accuracy and stability of detection. The RMSE and ARE values of Cr and Cu elements in the samples with a surface hardness of 98HA are less than 43HA and 70HA, and the R^2 is also larger, indicating that the detection accuracy of elements in the

sample with high surface hardness is higher. On the contrary, the value of the RSD increases with the increase of sample surface hardness, which represents the stability of test results decrease. This may be because the increase of sample surface hardness intensifies the disordered state of particle collision in the plasma, resulting in increased fluctuation of each test result. At the same time, the fluctuation of background signal and noise signal also increases, which increases the LOD value of Cr and Cu elements. The research in this paper can provide theoretical support for reducing the influence of matrix effects on quantitative analysis

Declarations

Acknowledgments

This paper was supported by the National Key Scientific Instrument and Equipment Development of China(grant No.2014YQ120351), Department of Science and Technology of Jilin Province of China(grant No.20200403008SF).

References

1. R.X. Yi, X.Y. Yang, R. Zhou, J.M. Li, H.W. Yu, Z.Q. Hao, L.B. Guo, X.Y. Li, Y.F. Lu and X.Y. Zeng, Anal. Chem., 2018, 90(11) ,7080.
2. R.X. Yi, L.B. Guo, X.H. Zou, J.M. Li, Z.Q. Hao, X.Y. Yang, X.Y. Li, X.Y. Zeng and Y.F. Lu, Opt. Express, 2016, 24(3), 2607.
3. I. Rehan, M.A. Gondal and K. Rehan, Talanta, 2018, 182, 443.
4. J. Cunat, F.J. Fortes and J.J. Laserna, Anal. Chim. Acta, 2009, 633(1), 38.
5. Y. Ding, G.Y. Xia, H.W. Ji and X. Xiong, Anal. Methods, 2019, 11(29), 3657.
6. E.C. Ferreira, D. Milori, E.J. Ferreira, L. Santos, L. Martin-Neto and A. Nogueira, Talanta, 2011, 85(1), 435.
7. P.R. Villas-Boas, R.A. Romano, M. Franco, E.C. Ferreira, E.J. Ferreira, S. Crestana, and D. Milori, Geoderma, 2016, 263, 195.
8. L.B. Guo, D. Zhang, L.X. Sun, S.C. Yao, L. Zhang, Z.Z. Wang, Q.Q. Wang, H.B. Ding, Y. Lu, Z.Y. Hou and Z. Wang, Front. Phys. 2021, 16(2), 25.
9. G. Kim, J. Kwak, K.R. Kim, H. Lee, K.W. Kim, H. Yang and K. Park, J. Hazard. Mater. 2013, 263(2), 754.
10. Y.T. Huang, J.J. Lin, X.M. Lin and W.N. Zheng, J. Anal. At. Spectrom., 2021, 36(11), 2553.
11. G.S. Senesi and N. Senesi, Anal. Chim. Acta, 2016, 938, 7.
12. S.M. Zaytsev, I.N. Krylov, A.M. Popov, N.B. Zorov and T.A. Labutin, Spectrochim. Acta B, 2018, 140, 65.
13. T. Wang, M.J. He, T.T. Shen, F. Liu, Y. He, X.M. Liu and Z.J. Qiu, Spectrochim. Acta B, 2018, 149, 300.

14. G. Cristoforetti, A.D. Giacomo, Dell'Aglio, S. Legnaioli, E. Tognoni, V. Palleschi and N. Omenetto, Spectrochim. Acta B, 2010, 65(1), 86.
15. M. Momcilovic, J Petrovic, J Ciganovic, I. Cvijovic-Alagic, F. Koldzic, and S. Zivkovic, Plasma Chem. Plasma Process., 2020, 40(2), 499.
16. Z. Ramezanian, S.M.R. Darbani and A.E. Majd, Appl. Opt., 2017, 56(24), 6917.
17. J.S. Cowpe, R.D. Moorehead, D. Moser, J.S. Astin, S. Karthikeyan, S.H. Kilcoyne, G. Crofts and R.D. Pilkington, Spectrochim. Acta B, 2011, 66(3), 290.
18. S.M. Aberkane, A. Bendib, K. Yahiaoui, S. Boudjemai, S. Abdelli-Messaci, T. Kerdja, S.E. Amara and M.A. Harith, Appl. Surf. Sci., 2014, 301, 225.
19. M. Momcilovic, S. Zivkovic, J. Petrovic, I. Cvijovic-Alagic and J. Ciganovic, Appl. Phys. B, 2019, 125(11), 222.
20. H. Sattar, J. Shi, H. Ran, M. Imran, W. Ding, P.D. Gupta and H.B. Ding, Journal of Nuclear Materials, 2020, 540, 152389.
21. Z.A. Abdel-Salam, A.H. Galmed, E. Tognoni and M.A. Harith, Spectrochim. Acta B, 2007, 62(12), 1343.

Figures

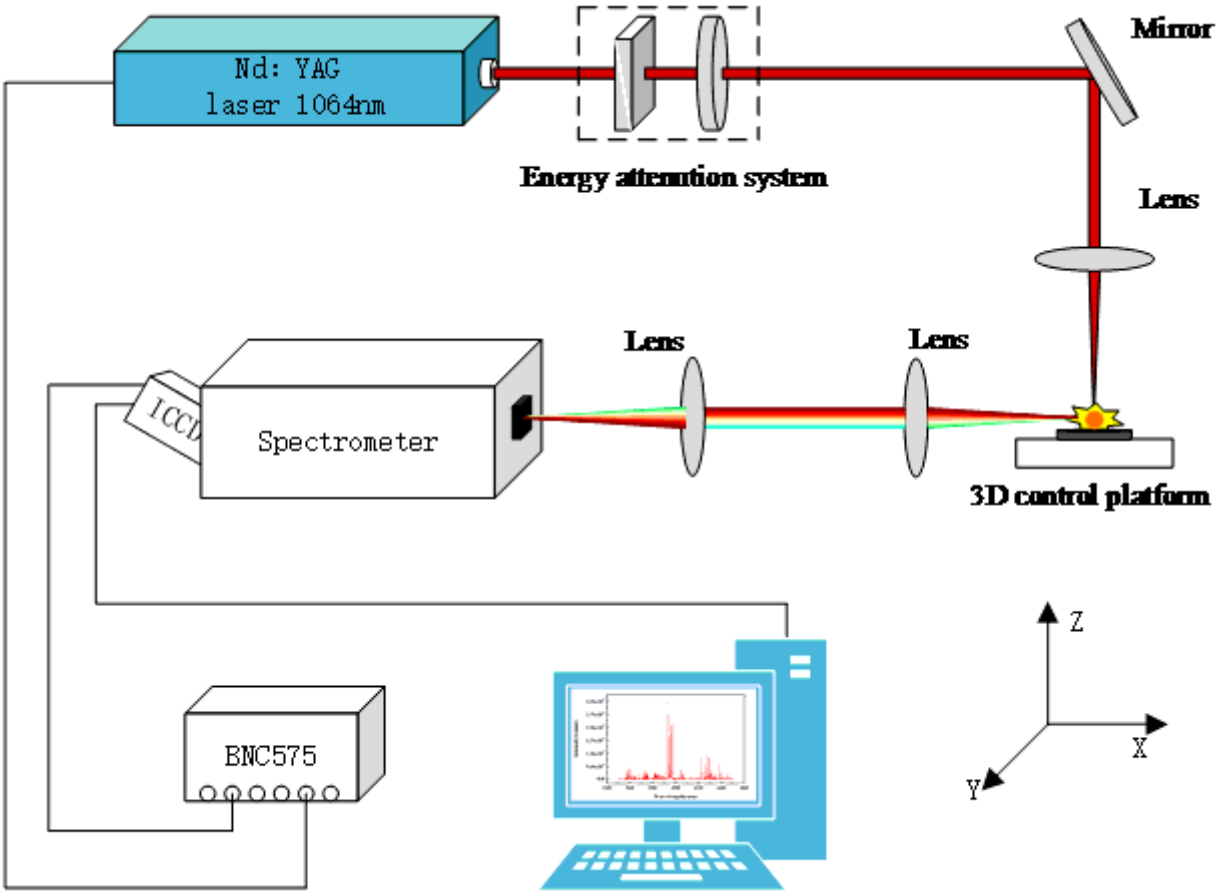

Figure 1

Schematic diagram of the experimental setup.

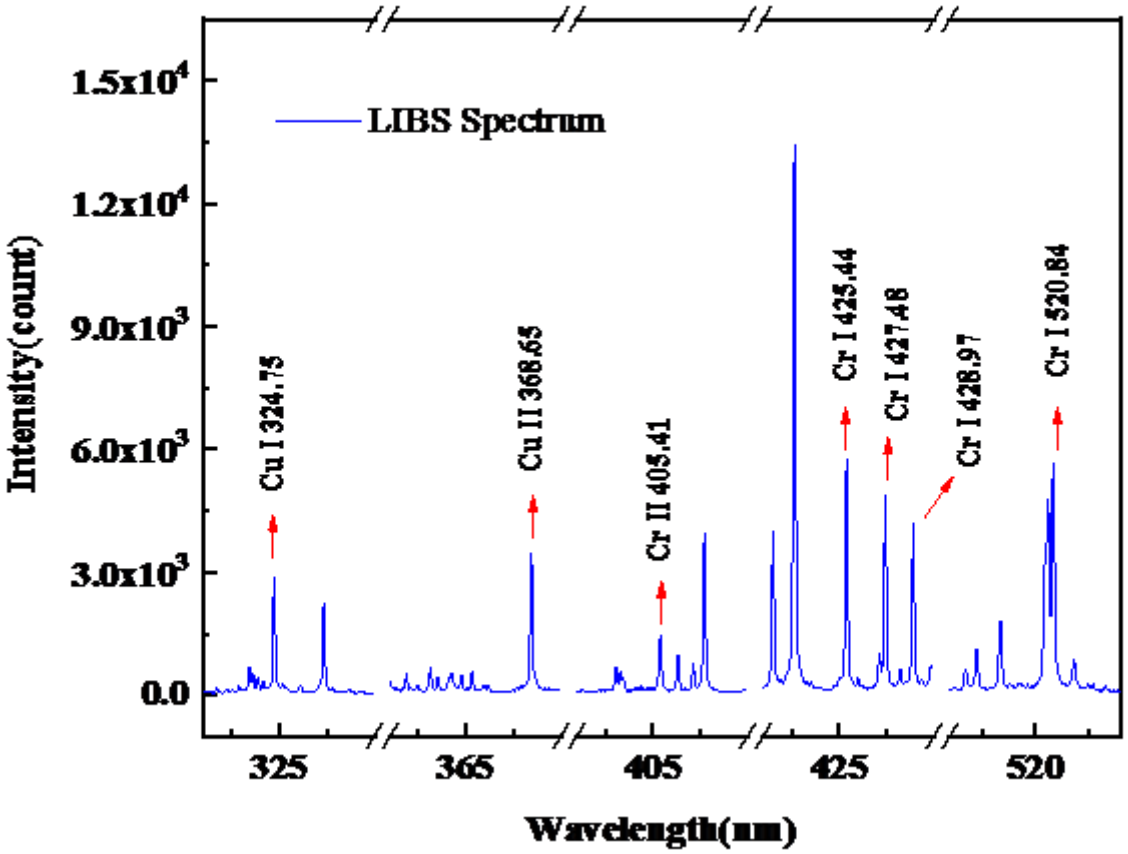

Figure 2

A spectrum in the experimental

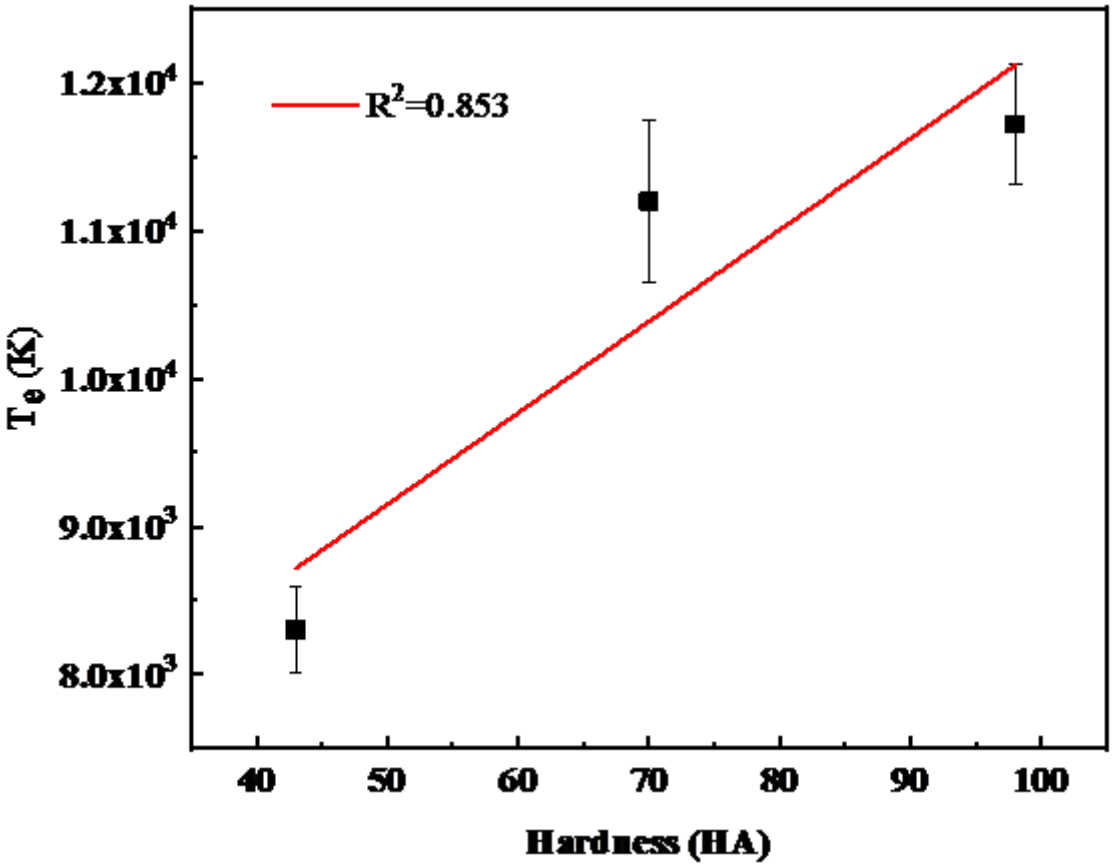

Figure 3

Relationship between plasma temperature and sample surface hardness.

Figure 4

Ablation craters diagram of samples with different surface hardness (a) 43HA, (b) 70HA, (c) 98HA.

Figure 5

Variation diagram of the ratio of ion line to atomic line with the surface hardness (a) Cr, (b) Cu.

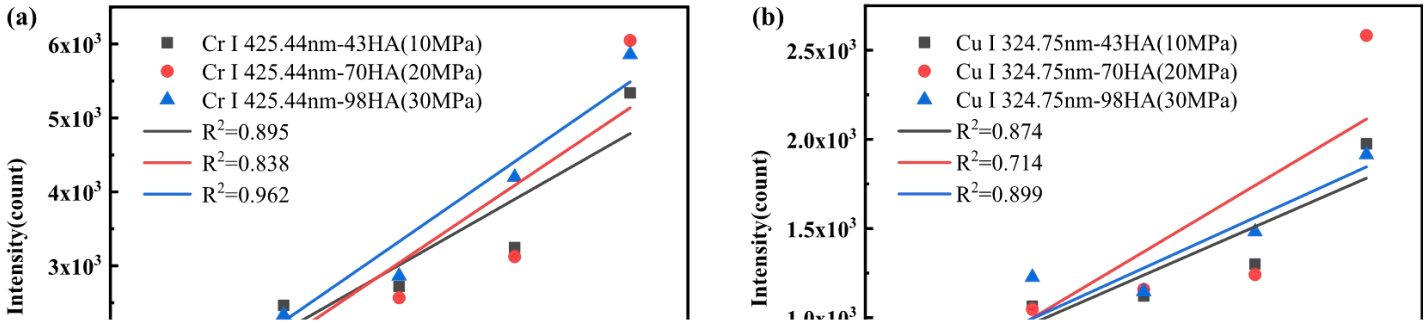

Figure 6

Calibration Curves of different surface hardness (a) Cr, (b) Cu.